ELSEVIER

Bioelectrochemistry and Bioenergetics 45 (1998) 3–16

BIOELECTROCHEMISTRY AND BIOENERGETICS

Time course of transmembrane voltage induced by time-varying electric fields—a method for theoretical analysis and its application

Tadej Kotnik *, Damijan Miklavčič, Tomaž Slivnik

University of Ljubljana, Faculty of Electrical Engineering, Tržaška 25, 1000 Ljubljana, Slovenia

Received 2 July 1997; revised 24 October 1997; accepted 27 October 1997

Abstract

The paper describes a general method for analysis of time courses of transmembrane voltage induced by time-varying electric fields. Using this method, a response to a wide variety of time-varying fields can be studied. We apply it to different field shapes used for electroporation and electrofusion: rectangular pulses, trapezoidal pulses (approximating rectangular pulses with finite rise time), exponential pulses, and sine(RF)-modulated pulses. Using the described method, the course of induced transmembrane voltage is investigated for each selected pulse shape. All the studies are performed at different pulse durations, each for both the normal physiological and the low-conductivity medium. For all the pulse shapes investigated, it is shown that as the conductivity of extracellular medium is reduced, this slows down the process of transmembrane voltage inducement. Thus, longer pulses have to be used to attain the desired voltage amplitude, as the influence of the fast, short-lived phenomena on the induced voltage is diminished. Due to this reason, RF-modulation in such a medium is ineffective. The appendix gives a complete set of derived expressions and a discussion about possible simplifications. © 1998 Elsevier Science S.A.

Keywords: Electric field stimulation; Transmembrane voltage; Pulse shape; Pulse duration; Electroporation; Low-conductivity medium

1. Introduction

Exposure of a biological cell to electric field can produce a variety of profound biochemical and physiological responses. Most of these responses are based on the modification of transmembrane voltage by the applied electric field [1–4]. If the field strength exceeds a certain threshold value, this can lead to pore formation in the membrane (electroporation) or fusion of adjacent cells (electrofusion) [5,6]. Nowadays, these phenomena are widely used in different applications, such as gene transfection [7], preparation of monoclonal antibodies in immunochemistry [8], and electrochemotherapy of tumors [9]. For optimal effects of such applications, one must select the appropriate shape, duration and amplitude of the applied electric field. This is only possible if the dynamics of transmembrane voltage induced by such a field can be evaluated.

If a spherical cell with no surface charge is exposed to a DC field, the steady-state value of transmembrane voltage $\Delta\Phi_m$ is calculated by solving the Laplace partial differential equation, which governs static electric fields and reflects their conservative properties. This approach yields the solution in form of the expression:

$$\Delta\Phi_m = fER\cos\theta \tag{1}$$

where E is the strength of the electric field (which has to be DC for this expression to be valid), R is the cell radius, θ is the polar angle measured with respect to the direction of the field, and f is a function reflecting the electrical and geometrical properties of the cell [10]:

$$f = \frac{3\lambda_o\left[3dR^2\lambda_i + (3d^2R - d^3)(\lambda_m - \lambda_i)\right]}{2R^3(\lambda_m + 2\lambda_o)\left(\lambda_m + \frac{1}{2}\lambda_i\right) - 2(R-d)^3(\lambda_o - \lambda_m)(\lambda_i - \lambda_m)} \tag{2}$$

where λ_i, λ_m and λ_o are the conductivities of the cytoplasm, cell membrane, and extracellular medium, respectively, R is

* Corresponding author. Tel.: +386-1-4768-768; fax: +386-1-4264-658; e-mail: tadej.kotnik@fe.uni-lj.si

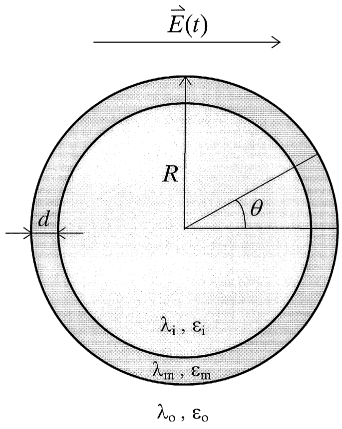

Fig. 1. The model on which the calculations were based. The cell is a sphere with radius of R, enclosed by a membrane of uniform thickness d. External electric field is homogeneous and retains its orientation, though its strength E changes with time. Specific conductivities and permittivities are attributed to regions occupied by cytoplasm (λ_i, ε_i), membrane (λ_m, ε_m) and extracellular medium (λ_o, ε_o).

again the cell radius, and d is the membrane thickness. The meaning of the parameters used in Eq. (2) is also illustrated in Fig. 1.

Often, a further simplification is made by assuming $\lambda_m \ll \lambda_i, \lambda_o$, which reduces function f into a constant, $f = 3/2$.

To analyze $\Delta\Phi_m$ in response to a step turn-on of a DC field, Eq. (1) is sometimes modified, presuming the exponential shape of the $\Delta\Phi_m$ in response to a step change of E:

$$\Delta\Phi_m(t) = fER\cos\theta\left[1 - \exp\left(-\frac{t}{\tau}\right)\right] \tag{3}$$

where τ is the time constant of the membrane given by Ref. [11]:

$$\tau = \frac{Rc_m}{\dfrac{2\lambda_o\lambda_i}{2\lambda_o + \lambda_i} + \dfrac{R}{d}\lambda_m} \tag{4}$$

and $c_m = \varepsilon_m/d$ is the membrane capacitance, with ε_m denoting the membrane permittivity.

The described time constant approach can also be used in the case of rectangular pulses, since the turn-off of the electric field is again a step change. However, electric fields with shapes different from rectangular, such as exponential, or RF-modulated, are often used. In these cases, a different approach to the evaluation is needed.

In this paper, we present a general method for analysis of time courses of transmembrane voltage induced by time-varying fields, and we use this method to study the fields commonly used for electroporation and electrofusion: single rectangular pulses, trapezoidal pulses (modeling rectangular pulses with rise time), exponential pulses, RF-modulated pulses, as well as trains of such pulses.

Two remarks should be made before we proceed with the discussion of the problem. First, since f and τ are actually functions, more rigorous rules of denotation would demand to imply this by writing the terms as $f(\lambda_i, \lambda_m, \lambda_o, R, d)$ and $\tau(\lambda_i, \lambda_m, \lambda_o, \varepsilon_m, R, d)$. For brevity, we avoid such denotation. Secondly, the calculations which lead to the described equations are based on two assumptions: (A) cell shape is presumed to be spherical; for a majority of cell types in a suspension, this is a fair approximation, but it does not hold for disc-shaped (e.g., erythrocytes) and rod-shaped cells (e.g., some types of bacteria); and (B) applied electric field is treated as homogeneous and defined as the ratio between the applied voltage and the distance between the electrodes; this approximation is only valid if two parallel plates are used as electrodes, and the distance between the plates is much smaller than the size of the plates; often, wire electrodes are used instead (e.g., needle electrodes in poration of tissues in vivo), yielding a strongly nonuniform distribution of the field, which can only be evaluated by means of numerical methods [12]. The two assumptions given by (A) and (B) provide the access to the analytical approach and shall therefore be retained in the forthcoming calculations.

2. Calculations

For the cases where electric field strength remains constant once the field is turned on, Eq. (1) can be used to give the steady-state solution. If cytoplasm, membrane and extracellular medium were all purely conductive (having no dielectric permittivity), this equation would also yield transmembrane voltage induced at any given moment in response to the momentary value of electric field strength. Any material, however, demonstrates a certain amount of permittivity. [1] When it is exposed to electric field, voltage induced on the material consists of two components; the first (due to the conductivity of the material) is proportional to the electric field strength, while the other (due to the permittivity of the material) is proportional to the time derivative of electric field strength [13]. In order to account for these permittivities, instead of conductivities of the materials, the more general *admittivity operators* have to be used:

$$\Lambda = \lambda + \varepsilon \frac{\mathrm{d}}{\mathrm{d}t} \tag{5}$$

where $\mathrm{d}/(\mathrm{d}t)$ is a differential operator that transforms a differentiable function $y(t)$ into its time derivative $(\mathrm{d}y)/(\mathrm{d}t)$.

By taking the function f and substituting Λ_i, Λ_m, and Λ_o for λ_i, λ_m, and λ_o, respectively, we obtain the following expression:

$$F = \frac{3\Lambda_\mathrm{o}\left[3dR^2\Lambda_\mathrm{i} + (3d^2R - d^3)(\Lambda_\mathrm{m} - \Lambda_\mathrm{i})\right]}{2R^3(\Lambda_\mathrm{m} + 2\Lambda_\mathrm{o})\left(\Lambda_\mathrm{m} + \frac{1}{2}\Lambda_\mathrm{i}\right) - 2(R-d)^3(\Lambda_\mathrm{o} - \Lambda_\mathrm{m})(\Lambda_\mathrm{i} - \Lambda_\mathrm{m})}. \tag{6}$$

F is a function of three differential operators (Λ_i, Λ_m, and Λ_o) and can thus itself be treated as a structured, higher-order differential operator [14]. To avoid dealing with differential operators, we transfer the analysis into complex-frequency space, where time derivatives are replaced by multiplication by the complex frequency (denoted by s). Here, the admittivity operator is formulated as:

$$\Lambda = \lambda + \varepsilon s. \tag{7}$$

If the terms Λ_i, Λ_m, and Λ_o in Eq. (6) are written according to Eq. (7), and the result is then expanded, we get the expression of the following type:

$$F(s) = \frac{a_1 s^2 + a_2 s + a_3}{b_1 s^2 + b_2 s + b_3} \tag{8}$$

where

$$a_1 = 3d\lambda_\mathrm{o}\left(\lambda_\mathrm{i}(3R^2 - 3dR + d^2) + \lambda_\mathrm{m}(3dR - d^2)\right), \tag{9a}$$

$$a_2 = 3d\left((\lambda_\mathrm{i}\varepsilon_\mathrm{o} + \lambda_\mathrm{o}\varepsilon_\mathrm{i})(3R^2 - 3dR + d^2) + (\lambda_\mathrm{m}\varepsilon_\mathrm{o} + \lambda_\mathrm{o}\varepsilon_\mathrm{m})(3dR - d^2)\right), \tag{9b}$$

$$a_3 = 3d\varepsilon_\mathrm{o}\left(\varepsilon_\mathrm{i}(3R^2 - 3dR + d^2) + \varepsilon_\mathrm{m}(3dR - d^2)\right), \tag{9c}$$

$$b_1 = 2R^3(\lambda_\mathrm{m} + 2\lambda_\mathrm{o})\left(\lambda_\mathrm{m} + \frac{1}{2}\lambda_\mathrm{i}\right) + 2(R-d)^3(\lambda_\mathrm{m} - \lambda_\mathrm{o})(\lambda_\mathrm{i} - \lambda_\mathrm{m}), \tag{9d}$$

$$b_2 = 2R^3\left(\lambda_\mathrm{i}\left(\frac{1}{2}\varepsilon_\mathrm{m} + \varepsilon_\mathrm{o}\right) + \lambda_\mathrm{m}\left(\frac{1}{2}\varepsilon_\mathrm{i} + 2\varepsilon_\mathrm{m} + 2\varepsilon_\mathrm{o}\right) + \lambda_\mathrm{o}(\varepsilon_\mathrm{i} + 2\varepsilon_\mathrm{m})\right) + 2(R-d)^3 \times\left(\lambda_\mathrm{i}(\varepsilon_\mathrm{m} - \varepsilon_\mathrm{o}) + \lambda_\mathrm{m}(\varepsilon_\mathrm{i} - 2\varepsilon_\mathrm{m} + \varepsilon_\mathrm{o}) - \lambda_\mathrm{o}(\varepsilon_\mathrm{i} - \varepsilon_\mathrm{m})\right), \tag{9e}$$

$$b_3 = 2R^3(\varepsilon_\mathrm{m} + 2\varepsilon_\mathrm{o})\left(\varepsilon_\mathrm{m} + \frac{1}{2}\varepsilon_\mathrm{i}\right) + 2(R-d)^3(\varepsilon_\mathrm{m} - \varepsilon_\mathrm{o})(\varepsilon_\mathrm{i} - \varepsilon_\mathrm{m}). \tag{9f}$$

In the same manner as function f would be more consistently denoted as $f(\lambda_\mathrm{i}, \lambda_\mathrm{m}, \lambda_\mathrm{o}, R, d)$, function F should be written as $F(\lambda_\mathrm{i}, \lambda_\mathrm{m}, \lambda_\mathrm{o}, \varepsilon_\mathrm{i}, \varepsilon_\mathrm{m}, \varepsilon_\mathrm{o}, R, d, s)$, thus, implying its dependence on all of these parameters. Again, for the brevity, we choose to explicitly indicate only the dependence of F on s (since this is the only dynamic parameter for a single

[1] The term ‘permittivity’ implies the total permittivity of the material, i.e., the product of the relative permittivity of the material (e.g., $\varepsilon_{\mathrm{r\ water}} = 81$) and the dielectric constant of the vacuum ($\varepsilon_\mathrm{o} = 8.854 \times 10^{-12}$ A s V^{-1} m^{-1}).

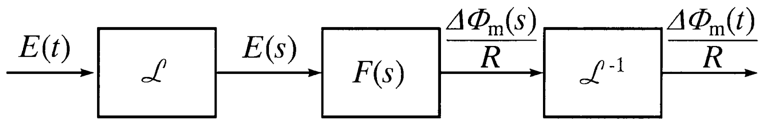

Fig. 2. The general principle used in the calculation of $\Delta\Phi_m(t)$ induced by $E(t)$. $\mathscr{L}$ represents the Laplace transform, and $\mathscr{L}^{-1}$ the inverse Laplace transform. $E(t)$ is first transformed into $E(s)$, which is then multiplied by $F(s)$ to give $\Delta\Phi_m(s)/R$. The normalized time course $\Delta\Phi_m(t)/R$ is then obtained as the inverse transform.

calculation—for other parameters, numerical values are inserted). Based on Eq. (1) and the introduced modifications, the relation between E and $\Delta\Phi_m$ in the complex-frequency space is given by:

$$\Delta\Phi_m(s) = F(s)\,E(s)\,R\cos\theta \quad (10)$$

where $\Delta\Phi_m(s)$ and $E(s)$ are Laplace (Heaviside) transforms of the time courses $\Delta\Phi_m(t)$ and $E(t)$, respectively, and $F(s)$ is given by Eq. (7).

The described approach allows the induced transmembrane voltage to be calculated for any time course $E(t)$, provided that it can be transformed into the complex-frequency space (i.e., provided that its Laplace transform $E(s)$ exists). The product $F(s)E(s)$ represents $\Delta\Phi_m(s)$ at $\theta = 0$, normalized to the cell radius, and the inverse Laplace transform yields $\Delta\Phi_m(t)$ at $\theta = 0$, normalized to R. The concept of the method is sketched in Fig. 2. One then multiplies the expression by R to scale the response, and by $(\cos\theta)$ to obtain the spatial distribution of induced transmembrane voltage.

General solutions describing responses to rectangular, triangular, trapezoidal, exponential, and sine(RF)-modulated pulses are given in Appendix A. In Section 3, we focus on specific time courses obtained from these solutions by insertion of numerical values of the parameters.

The cosine distribution of $\Delta\Phi_m$ on the cell membrane is retained in all cases and at any moment. Therefore, the multiplicative term $(\cos\theta)$ will be left out in further analysis (thus, we study $\Delta\Phi_m$ at $\theta = 0$). Also, for the clarity of reasoning, values of the geometrical (R and d) and electrical parameters (λ_i, λ_m, ε_i, ε_m, and ε_o) will be kept constant throughout the analysis. The only exception will be made for the extracellular medium conductivity (λ_o). While the permittivity of the extracellular medium is mostly dictated by its prevalent constituent, i.e., water, the medium conductivity strongly depends on the ionic concentrations in the medium. Since in different reports of experiments in vitro conductivity of the medium varies for at least two orders of magnitude [15–17], we will consider two particular cases—a physiological medium (with $\lambda_o \sim \lambda_i$) and a typical low-conductivity medium ($\lambda_o \ll \lambda_i$). Values of all the parameters are given in Table 1.

Table 1
Values of electric and dimensional parameters used in the calculations

Parameter	Denotation	Value
Cytoplasmic conductivity	λ_i	3.0×10^{-1} S m^{-1} [a]
Cytoplasmic permittivity	ε_i	7.1×10^{-10} A s V^{-1} m^{-1} [b]
Membrane conductivity	λ_m	3.0×10^{-7} S m^{-1} [c,d]
Membrane permittivity	ε_m	4.4×10^{-11} A s V^{-1} m^{-1} [e]
Extracellular medium conductivity	λ_o	3.0×10^{-1} S m^{-1} (physiological medium)[f], 1.0×10^{-2} S m^{-1} (low-conductivity medium)[g]
Extracellular medium permittivity	ε_o	7.1×10^{-10} A s V^{-1} m^{-1} [b]
Cell radius	R	10 μm[h]
Membrane thickness	d	5 nm[h]

[a] Reported values range between 2.0×10^{-1} S m^{-1} and 5.5×10^{-1} S m^{-1} [18–20].
[b] A typical permittivity of an aqueous solution (relative permittivity ≈ 80).
[c] Gascoyne et al. [21].
[d] From Hu et al. [22], using conversion method given by Arnold et al. [17].
[e] Measured values of relative membrane permittivity lie between 4.5 and 6.5 [21]; relative membrane permittivity of 5 corresponds to $\varepsilon_m \approx 4.4\times10^{-11}$ A s V^{-1} m^{-1}; a similar result is obtained from the data on membrane capacitance—from $c_m \approx 10^{-2}$ F m^{-2} [17,23,22,24] we get $\varepsilon_m = c_m d \approx 5.0\times10^{-11}$ A s V^{-1} m^{-1}.
[f] Set at equal value as λ_i.
[g] Reported values range from 1.0×10^{-3} S m^{-1} to 5.0×10^{-2} S m^{-1} [17,25–27]; many authors do not give the value of λ_o.
[h] Alberts et al. [28].

3. Results and discussion

3.1. Rectangular pulses

Rectangular pulses are often used in electroporation and electrofusion [15,29,30]. It is sensible to first focus on $\Delta\Phi_m(t)$ induced by an ideal rectangular pulse, thus, elucidating the effect of electrical properties of the medium on the relation between $E(t)$ and $\Delta\Phi_m(t)$. Then, by accounting for rise time of the pulse produced by a realistic generator, we can also analyze the role of generator features.

The derivation of $\Delta\Phi_m(t)$ in response to an ideal rectangular pulse is given by Eq. (A7) in Appendix A. Fig. 3 shows time courses of $\Delta\Phi_m$ induced by three rectangular pulses with durations of 200 ns, 1 μs, and 5 μs, respectively, each of them plotted for both a physiological and a low conductivity medium.

Fig. 3 shows that the induced transmembrane voltage is formed much slower when the medium conductivity is low. Pulses longer than 10 μs, however, suffice for $\Delta\Phi_m$ to reach the steady-state value even in a low conductivity medium. With such pulses, for a purpose of only evaluating this steady-state value (which still depends on the conductivities and dimensions of the cell), the simpler Eq. (1) can be used.

3.2. Trapezoidal pulses (rectangular pulses with rise time)

Pulses produced by a realistic generator are always characterized by a certain rise time. To account for this, we presumed the trapezoidal shape of the generated pulse (this is certainly a simplification, since the course of $E(t)$ during the rise time is generally nonlinear). The time course of $\Delta\Phi_m$ in response to a trapezoidal pulse is given by Eq. (A11) in Appendix A. Since rise times of modern pulse generators never exceed several tenths of a microsecond, and the induced $\Delta\Phi_m$ only reaches a very small fraction of its final value during such a short time (presuming that the pulse duration is long enough to obtain a substantial response, e.g., case (c) in Fig. 3), the response induced by a trapezoidal pulse with such a short rise time is practically equivalent to the response induced by a rectangular pulse of the same duration. Setting the pulse duration significantly longer than the rise time is the only sensible choice if the pulse is to resemble a rectangular shape, which is generally desired.

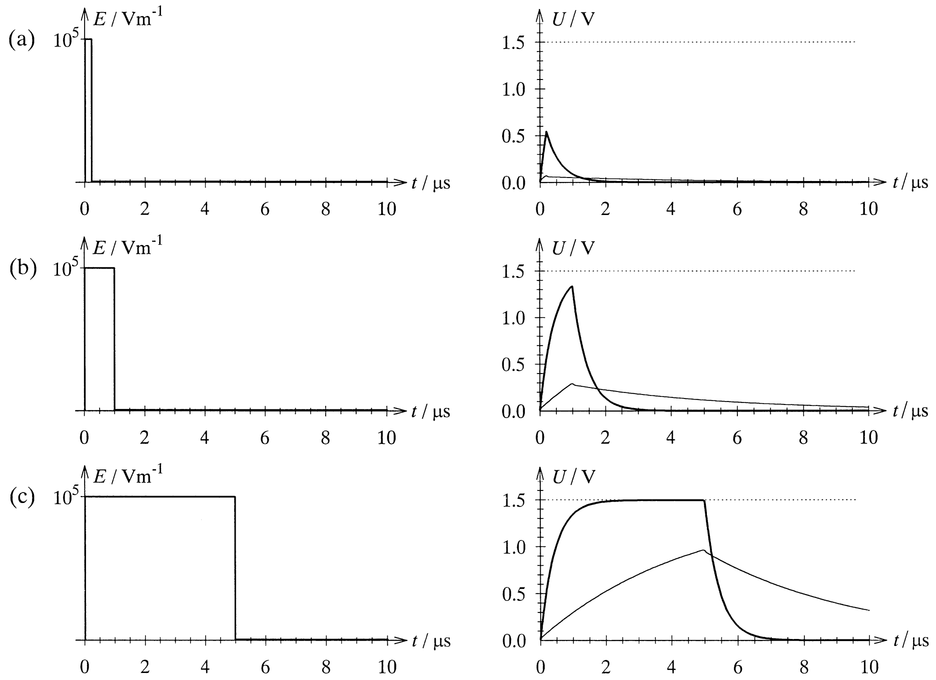

Fig. 3. A rectangular pulse (left) and the induced $\Delta\Phi_m(t)$ (right). (a) $T_1 = 200$ ns; (b) $T_1 = 1$ μs; (c) $T_1 = 5$ μs. The thicker line corresponds to the response in a physiological medium, and the thinner line to the response in a low-conductivity medium. The dotted line gives the value of $3/2$ ER (the steady-state value of $\Delta\Phi_m$, at $\theta = 0$, according to the most simplified relation between E and $\Delta\Phi_m$, see Eq. (2) and the subsequent commentary). For parameter values used in the calculations, see Table 1.

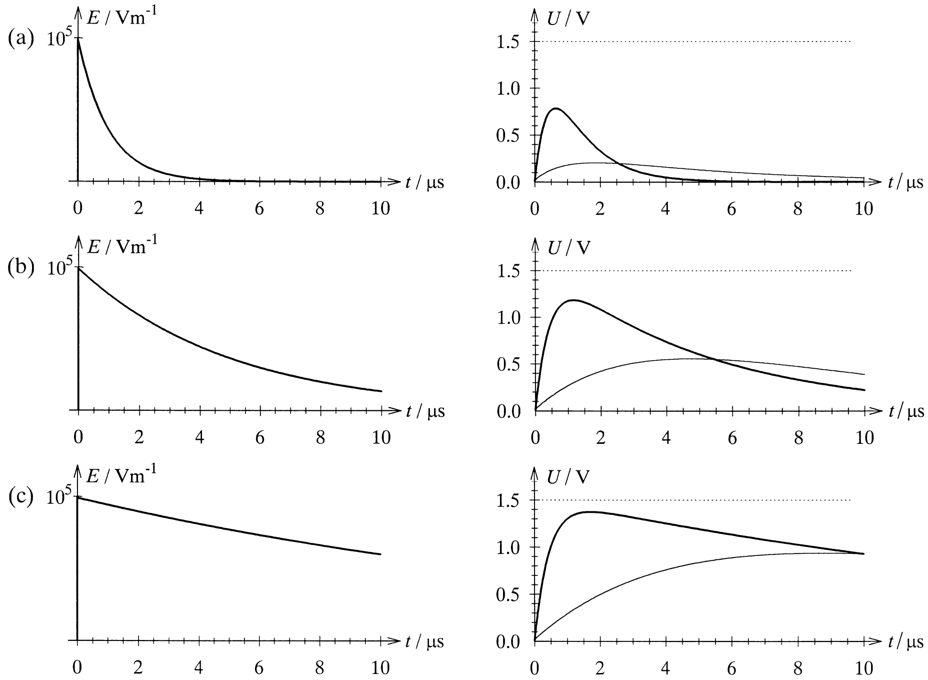

Fig. 4. An exponential pulse (left) and the induced $\Delta\Phi_m(t)$ (right). (a) $\tau_p = 1$ μs; (b) $\tau_p = 5$ μs; (c) $\tau_p = 20$ μs. The thicker line corresponds to the response in a physiological medium, and the thinner line to the response in a low-conductivity medium. The dotted line gives the value of $3/2$ ER.

3.3. Exponential pulses

Exponentially decaying pulses are also widespread in the applications [31–33]. Since the inducement process is not instantaneous, it is obvious that with pulses of this shape, neither the steady-state Eq. (1), nor the first-order response given by Eq. (3) enables the evaluation of the induced voltage. The derivation of $\Delta\Phi_m(t)$ in response to an exponential (exponentially decaying) pulse is given by Eq. (A12d) in Appendix A. Fig. 4 shows time courses of $\Delta\Phi_m$ induced by three such pulses, with time constants of 1 μs, 5 μs, and 20 μs, respectively, each of the responses plotted for both a physiological and a low conductivity medium.

Because the exponential pulses are inherently time-varying, the influence of pulse duration (determined here by the time constant of the pulse) on the shape of $\Delta\Phi_m$ and its maximum value is probably most apparent with this type of pulses. Typical time constants of the pulses used in experiments lie in the range of ms, and focusing on the range of first several μs of such pulse, provided that the physiological medium is used, the pulse resembles a rectangular pulse. Therefore, we can evaluate the peak value of the induced voltage using the Eq. (1) without any crucial inaccuracy. On the other hand, a decrease in medium conductivity slows the inducement process significantly. As Fig. 4 shows, it is generally very hard to

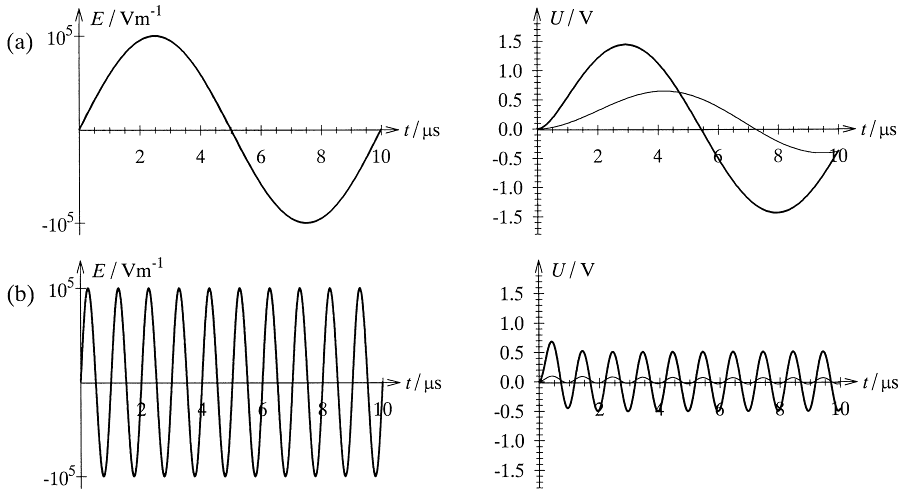

Fig. 5. A sine wave (left) and the induced $\Delta\Phi_m(t)$ (right). (a) $\omega/2\pi = 100$ kHz; (b) $\omega/2\pi = 1$ MHz. The thicker line corresponds to the response in a physiological medium, and the thinner line to the response in a low-conductivity medium.

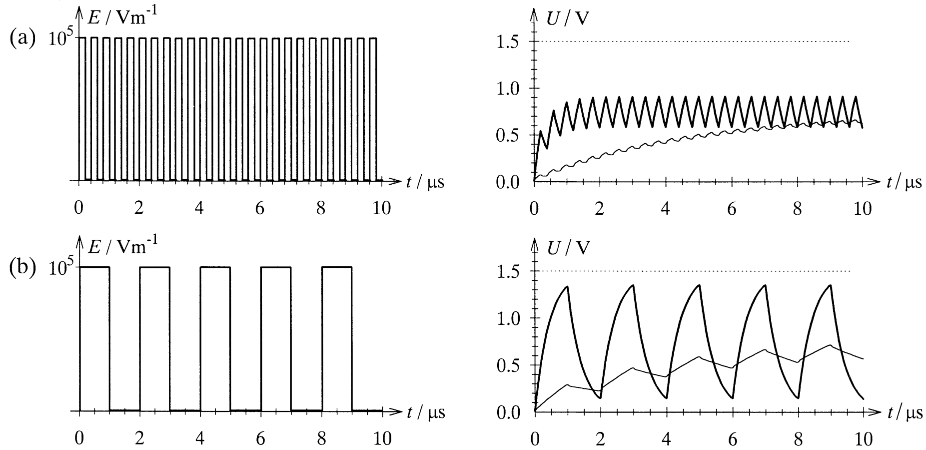

Fig. 6. A train of rectangular pulses (left) and the induced $\Delta\Phi_m(t)$ (right). (a) $T_1 = 200$ ns, $T_2 = 400$ ns; (b) $T_1 = 1$ μs, $T_2 = 2$ μs. The thicker line corresponds to the response in a physiological medium, and the thinner line to the response in a low-conductivity medium. The dotted line gives the value of $3/2$ ER.

predict the peak value of the induced voltage, since the shape of the response strongly depends on the medium conductivity (it is influenced by other parameters as well).

3.4. Sine-modulated pulses

In the recent years, several papers have reported an improved efficiency of electroporation and electrofusion obtained by modulation of rectangular pulses with a radio-frequency sinewave [34,35]. Without getting involved in the discussion about the mechanisms of improved efficiency, we present the analysis of the time courses of $\Delta\Phi_m$ induced by a sine-shaped electric field. Since the response induced by a modulated pulse is a combination of responses to a rectangular pulse and to a sine wave, the effect of the latter component is best studied separately. The derivation of $\Delta\Phi_m(t)$ in response to a sine wave is given by Eq. (A14d) in Appendix A, while the response to a sine-modulated rectangular pulse is derived in Eq. (A16). Fig. 5 shows time courses of $\Delta\Phi_m$ induced by two sine waves with frequencies of 100 kHz and 1 MHz, respectively. Each response is plotted for both a physiological and a low conductivity medium.

We see that with increasing frequency, the amplitude of the induced $\Delta\Phi_m$ decreases. Since the low conductivity medium slows down the dynamics of voltage inducement, the attenuation of the oscillations in the induced transmembrane voltage occurs at much lower frequencies. Therefore, the efficacy of modulation in such a medium is questionable.

3.5. Trains of pulses

When trains of pulses are applied, the gap between consecutive pulses is in most cases much larger than the pulse duration. Therefore, the transmembrane voltage induced by a pulse practically disappears before the next pulse occurs. Response to each pulse is dictated by this pulse only and can be treated separately from the responses to other pulses. The gap between pulses can, however, be decreased to such an extent that the next pulse starts before the response to the previous one completely fades away. In this case, the impact of superposition of single responses becomes evident. Fig. 6 shows two examples of responses to such trains of rectangular pulses.

4. Conclusions

Besides providing a tool for general analysis of time courses of transmembrane voltage induced by different time-varying electric fields, the presented method allows to calculate a particular response to a pulse of given shape and duration, time constant, or modulation frequency. In this manner, the method can be used when deciding on the pulse parameters that would provide a specific value of induced transmembrane voltage and (or) retain this value for a specific duration.

There is another important (though at the present time still hypothetical) utilization of the presented method. As the computer capabilities increase, molecular dynamics simulations of lipid bilayers promise to reach time ranges of microseconds within several years [36]. Since the time of pore formation in electroporation is also estimated to lie within the microsecond range [15,37], the opportunity could soon arise to simulate electroporation on a molecular level. For such a simulation to yield realistic results, it is essential to model all the details as authentically as possible, including exact time course of transmembrane voltage induced by a given pulse of electric field strength.

One of the important conclusions of this study is the necessity to determine the conductivity of the medium used in a particular experiment. This conductivity strongly influences the dynamics of induced transmembrane voltage, and hence

Table 2
Critical values of pulse parameters

Pulse type	Parameter	Critical value	Explanation
Rectangular	Pulse duration	$< 1\ \mu s$[a] $< 13\ \mu s$[b]	Induced voltage does not reach 90% of the steady-state value predicted by $\Delta\Phi_m = 3/2\ ER\cos\theta$
Exponential	Time constant	$< 20\ \mu s$[a] $< 260\ \mu s$[b]	Induced voltage does not reach 90% of the steady-state value predicted by $\Delta\Phi_m = 3/2\ ER\cos\theta$
Sine-modulated	Sine frequency	> 170 kHz[a] > 14 kHz[b]	Amplitude ratio between the offset and the sine in $\Delta\Phi_m(t)$ falls below 90% of the same ratio in $E(t)$
		> 5.5 MHz[a] > 600 kHz[b]	Amplitude ratio between the offset and the sine in $\Delta\Phi_m(t)$ falls below 10% of the same ratio in $E(t)$

[a] Physiological medium ($\lambda_o = 3.0\times10^{-1}$ S m^{-1}).
[b] Low conductivity medium ($\lambda_o = 1.0\times10^{-2}$ S m^{-1}); other values used in this estimation are given in Table 1.

imposes the range of pulse duration (and, though to less extent, the pulse amplitude; a thorough treatise of this problem is given in Ref. [10]). Fig. 5 gives an illustrative example of this influence, as the use of low conductivity medium practically eliminates the response to a 1 MHz sine wave.

Generally, each pulse shape is characterized by a key parameter (e.g., pulse duration, time constant, or sine frequency). One can define a certain critical value of this parameter, above (or below) which the differences between the steady-state results (given by Eq. (1)) and the dynamic analysis (based on the expressions for the time courses given in Appendix A) become obvious. Table 2 gives the key parameters of investigated pulse shapes and the estimations of pertaining critical values for both physiological and low conductivity medium.

Another very important value to bear in mind when designing the pulses for electroporation or electrofusion is the radius of the cells used in the experiment, since the amplitude of induced transmembrane voltage strongly depends on cell radius, [2] as Eqs. (6) and (10) reveal.

Finally, we should also mention that the presented model, though already fairly complex, does not account for the fact that permittivity of any material is also frequency dependent. This dependence becomes apparent when components in the MHz range are present in the harmonic spectrum of $E(t)$ [38]. Some dielectrophoretic and electrorotational measurements imply that even in highly conductive extracellular solutions, very short pulses (or very high field frequencies) consistently induce lower transmembrane voltage than predicted theoretically [39,23]. If the model was expanded further by taking into account the frequency-dependent behavior of ε_i, ε_m, and ε_o, it might offer an explanation for these results.

Acknowledgements

This work was supported in part by the Ministry of Science and Technology of the Republic of Slovenia and by the Cellular Engineering Project (PECO Programme, Contract No. ERB-CIPA-CT 93-0235) of the European Community.

Appendix A

A.1. General principles

As shown in Fig. 2, three steps are necessary to obtain the time course of transmembrane voltage $\Delta\Phi_m(t)$ induced by a given time course of electric field strength $E(t)$. First, the Laplace transform of $E(t)$ is calculated:

$$E(s) = \mathscr{L}[E(t)] \tag{A1}$$

$\Delta\Phi_m(s)$ is then obtained as

$$\Delta\Phi_m(s) = E(s)\cdot F(s)\cdot R\cos\theta \tag{A2}$$

and the inverse Laplace transform of this expression yields the time course $\Delta\Phi_m(t)$:

$$\Delta\Phi_m(t) = \mathscr{L}^{-1}[\Delta\Phi_m(s)]. \tag{A3}$$

This method is useful for simple mathematical functions $E(t)$, for which both the Laplace transform and the inverse

[2] A first look at Eq. (10) might suggest that the amplitude of $\Delta\Phi_m$ is exactly proportional to R. This is not true, however, since $F(s)$ is also a function of R.

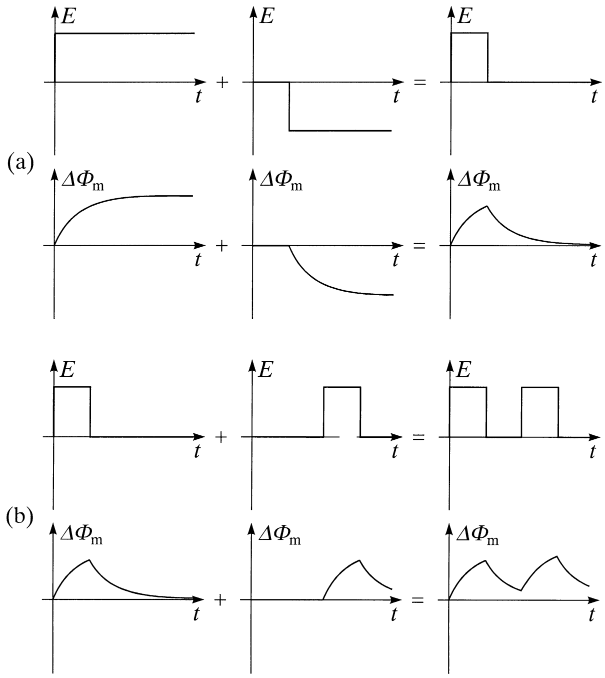

Fig. 7. An example of two consecutive applications of superposition principle. (a) Superposition of two oppositely signed step functions gives a rectangular pulse. Due to the linearity of the transforms, superposition of responses to these step functions yields a response to this rectangular pulse. (b) Superposition of shifted pulses yields a train of pulses, and superposition of responses to single pulses (which were constructed by the first superposition) results in the response to the train.

transform of corresponding $\Delta\Phi_m(t)$ given by Eq. (A2) are easily calculated. As for the more complex functions $E(t)$, many of them can be represented in the form of a linear combination of these simple functions:

$$E(t) = K_1 \cdot E_1(t) + K_2 \cdot E_2(t) + \ldots + K_n \cdot E_n(t). \tag{A4}$$

Since both the Laplace transform and the inverse Laplace transform are linear operations, the response $\Delta\Phi_m(t)$ induced by $E(t)$ which conforms to (Eq. (A4)) can be obtained as a sum of partial responses, i.e.,

$$\Delta\Phi_m(t) = K_1 \cdot \Delta\Phi_{m1}(t) + K_2 \cdot \Delta\Phi_{m2}(t) + \ldots + K_n \cdot \Delta\Phi_{mn}(t) \tag{A5}$$

where $\Delta\Phi_{mi}(t)$ denotes the response to $E_i(t)$ alone. Based on this property, $\Delta\Phi_m(t)$ induced by a rectangular pulse of amplitude E_0 and duration T can be calculated as a sum of two step responses bearing opposite signs, with amplitudes $+E_0$ and $-E_0$, the second step response delayed for T with respect to the first one. Similarly, a response to trapezoidal pulse of duration T and rise time T_{on} is obtained as a sum of four ramp responses, the last three shifted after the first one by T_{on}, $T - T_{on}$ (presuming thereby $T_{off} = T_{on}$), and T, respectively (the terms signed $+$, $-$, $-$, and $+$, respectively, for a positive pulse). Using the rules of linearity once again, we can take the obtained pulse response and consecutively superimpose an array of shifted pulse responses, thus determining the response to a series (train) of pulses. The described example of multilevel superposition is sketched in Fig. 7.

A.2. Rectangular pulses

We first calculate $\Delta\Phi_m(t)$ induced by the unit step function (we denote the step response by $\Delta\Phi_{m1}$):

$$E(t) = u_0(t) \tag{A6a}$$

$$E(s) = \frac{1}{s} \tag{A6b}$$

$$\frac{\Delta\Phi_{m1}(s)}{R} = F(s) \cdot E(s) = \frac{a_1 + a_2 s + a_3 s^2}{b_1 s + b_2 s^2 + b_3 s^3} \tag{A6c}$$

$$\frac{\Delta\Phi_{m1}(t)}{R} = \frac{a_3}{b_3}\cdot u_0(t) + \left[\frac{a_1}{2b_1} - \frac{a_3}{2b_3} + \frac{\frac{a_1 b_2}{2b_1} - a_2 + \frac{a_3 b_2}{2b_3}}{\sqrt{b_2^2 - 4b_1 b_3}}\right]\cdot\left(1 - e^{-\frac{t}{\tau_1}}\right)\cdot u_0(t)$$
$$+ \left[\frac{a_1}{2b_1} - \frac{a_3}{2b_3} - \frac{\frac{a_1 b_2}{2b_1} - a_2 + \frac{a_3 b_2}{2b_3}}{\sqrt{b_2^2 - 4b_1 b_3}}\right]\cdot\left(1 - e^{-\frac{t}{\tau_2}}\right)\cdot u_0(t). \qquad \text{(A6d)}$$

The constants from a_1 up to b_3 are given by Eqs. (9a), (9b), (9c), (9d), (9e) and (9f) in the main text, and the time constants τ_1 and τ_2 are given by:

$$\tau_1 = \frac{2b_3}{b_2 - \sqrt{b_2^2 - 4b_1 b_3}}, \qquad \text{(A6e)}$$

$$\tau_2 = \frac{2b_3}{b_2 + \sqrt{b_2^2 - 4b_1 b_3}}. \qquad \text{(A6f)}$$

We choose to represent the powers of the exponential parts in Eq. (A6d) in terms of τ_1 and τ_2, because the time constants given by Eqs. (A6e) and (A6f) characterize the responses to all the treated functions $E(t)$, as we shall see later.

Eq. (A6d) gives the response normalized to both the cell radius (R) and the amplitude of electric field strength (E). To obtain the actual response, the amplitude has to be scaled by both R and E. A closer look at Eq. (A6d) reveals that at $t \to 0$ the normalized response equals a_3/b_3, and with $t \to \infty$ it approaches a_1/b_1.

To obtain the response to a rectangular pulse, we combine two step responses, as described before and illustrated in Fig. 7:

$$\Delta\Phi_m(t) = \Delta\Phi_{m1}(t)\cdot u_0(t) - \Delta\Phi_{m1}(t - T_1)\cdot u_{T_1}(t) \qquad \text{(A7)}$$

where T_1 is the pulse duration.

Using the superposition principle once again, we can formulate the response to a train of pulses as:

$$\Delta\Phi_m(t) = \sum_{k=0}^{\infty}\left[\Delta\Phi_{m1}(t - kT_2)\cdot u_{kT_2}(t) - \Delta\Phi_{m1}((t - T_1) - kT_2)\cdot u_{T_1 + kT_2}(t)\right] \qquad \text{(A8)}$$

where T_1 is again the pulse duration, and T_2 is the pulse period (time elapsed between consecutive pulses). To evaluate the response in a finite time range, e.g., up to $t = T_{fin}$, one only has to evaluate the sum up to $k = T_{fin}/T_2$.

A.3. Triangular and trapezoidal pulses

To analyze the response to a triangular or a trapezoidal pulse, we first determine the response induced by the unit ramp function, denoting this response by $\Delta\Phi_{mt}(t)$:

$$E(t) = (t)\cdot u_0(t) \qquad \text{(A9a)}$$

$$E(s) = \frac{1}{s^2} \qquad \text{(A9b)}$$

$$\frac{\Delta\Phi_{mt}(s)}{R} = F(s)\cdot E(s) = \frac{a_1 + a_2 s + a_3 s^2}{b_1 s^2 + b_2 s^3 + b_3 s^4} \qquad \text{(A9c)}$$

$$\frac{\Delta\Phi_{mt}(t)}{R} = \frac{a_1}{b_1}\cdot t\cdot u_0(t) + \left[\frac{a_2}{2b_1} - \frac{a_1 b_2}{2b_1^2} + \frac{\frac{a_1 b_3}{b_1} + \frac{a_2 b_2}{2b_1} - \frac{a_1 b_2^2}{2b_1^2} - a_3}{\sqrt{b_2^2 - 4b_1 b_3}}\right]\cdot\left(1 - e^{-\frac{t}{\tau_1}}\right)\cdot u_0(t)$$
$$+ \left[\frac{a_2}{2b_1} - \frac{a_1 b_2}{2b_1^2} - \frac{\frac{a_1 b_3}{b_1} + \frac{a_2 b_2}{2b_1} - \frac{a_1 b_2^2}{2b_1^2} - a_3}{\sqrt{b_2^2 - 4b_1 b_3}}\right]\cdot\left(1 - e^{-\frac{t}{\tau_2}}\right)\cdot u_0(t) \qquad \text{(A9d)}$$

where the constants from a_1 up to b_3 are given by Eqs. (9a), (9b), (9c), (9d), (9e) and (9f) in the main text, while τ_1 and τ_2 are defined by Eqs. (A6e) and (A6f), respectively.

The response to a symmetrical triangular pulse of duration T_1 is then given by:

$$\Delta\Phi_{\mathrm{m}}(t)=\Delta\Phi_{\mathrm{m}t}(t)\cdot u_0(t)-2\cdot\Delta\Phi_{\mathrm{m}t}\left(t-\frac{T_1}{2}\right)\cdot u_{\frac{T_1}{2}}(t)+\Delta\Phi_{\mathrm{m}t}(t-T_1)\cdot u_{T_1}(t) \tag{A10}$$

whereas the response to a symmetrical trapezoidal pulse of duration T_1 and rise time T_{on} is expressed as:

$$\Delta\Phi_{\mathrm{m}}(t)=\Delta\Phi_{\mathrm{m}t}(t)\cdot u_0(t)-\Delta\Phi_{\mathrm{m}t}(t-T_{\mathrm{on}})\cdot u_{T_{\mathrm{on}}}(t)-\Delta\Phi_{\mathrm{m}t}(t-(T_1-T_{\mathrm{on}}))u_{T_1-T_{\mathrm{on}}}(t)+\Delta\Phi_{\mathrm{m}t}(t)(t-T_1)u_{T_1}(t). \tag{A11}$$

To obtain the response to a train of pulses, we gather a series of shifted pulse responses into a sum on the analogy of the principle presented by Eq. (A8).

A.4. Exponential pulses

For an exponentially decaying pulse with time constant τ_{p}, we denote the induced transmembrane voltage by $\Delta\Phi_{\mathrm{mexp}}(t)$ and compute:

$$E(t)=e^{-\frac{t}{\tau_{\mathrm{p}}}}\cdot u_0(t) \tag{A12a}$$

$$E(s)=\frac{1}{s+\frac{1}{\tau_{\mathrm{p}}}} \tag{A12b}$$

$$\frac{\Delta\Phi_{\mathrm{mexp}}(s)}{R}=F(s)\cdot E(s)=\frac{a_1+a_2s+a_3s^2}{(b_1+b_2s+b_3s^2)(s+\tau_{\mathrm{p}}^{-1})} \tag{A12c}$$

$$\begin{aligned}\frac{\Delta\Phi_{\mathrm{mexp}}(t)}{R}=&\left[\frac{a_1\tau_{\mathrm{p}}^2-a_2\tau_{\mathrm{p}}+a_3}{b_1\tau_{\mathrm{p}}^2-b_2\tau_{\mathrm{p}}+b_3}\right]\cdot e^{-\frac{t}{\tau_{\mathrm{p}}}}\cdot u_0(t)\\
&+\left[\frac{\left(\frac{a_3b_1}{b_3}-a_1\right)\cdot\tau_{\mathrm{p}}+a_2-\frac{a_3b_2}{b_3}}{2\cdot(b_1\tau_{\mathrm{p}}^2-b_2\tau_{\mathrm{p}}+b_3)}+\frac{\left(a_2b_1-\frac{a_1b_2}{2}-\frac{a_3b_1b_2}{2b_3}\right)\cdot\tau_{\mathrm{p}}+a_1b_3-a_3b_1-\frac{a_2b_2}{2}+\frac{a_3b_2^2}{2b_3}}{(b_1\tau_{\mathrm{p}}^2-b_2\tau_{\mathrm{p}}+b_3)\sqrt{b_2^2-4b_1b_3}}\right]\\
&\cdot\tau_{\mathrm{p}}\cdot e^{-\frac{t}{\tau_1}}\cdot u_0(t)\\
&+\left[\frac{\left(\frac{a_3b_1}{b_3}-a_1\right)\cdot\tau_{\mathrm{p}}+a_2-\frac{a_3b_2}{b_3}}{2\cdot(b_1\tau_{\mathrm{p}}^2-b_2\tau_{\mathrm{p}}+b_3)}-\frac{\left(a_2b_1-\frac{a_1b_2}{2}-\frac{a_3b_1b_2}{2b_3}\right)\cdot\tau_{\mathrm{p}}+a_1b_3-a_3b_1-\frac{a_2b_2}{2}+\frac{a_3b_2^2}{2b_3}}{(b_1\tau_{\mathrm{p}}^2-b_2\tau_{\mathrm{p}}+b_3)\sqrt{b_2^2-4b_1b_3}}\right]\\
&\cdot\tau_{\mathrm{p}}\cdot e^{-\frac{t}{\tau_2}}\cdot u_0(t).\end{aligned} \tag{A12d}$$

This solution already gives a response to an exponential pulse. To obtain a response to a train of exponential pulses, we again follow the logic presented by Eq. (A8), only this time the expression is even simpler. For a pulse period T_2, it reads:

$$\Delta\Phi_{\mathrm{m}}(t)=\sum_{k=0}^{\infty}\Delta\Phi_{\mathrm{mexp}}(t-kT_2)u_{kT_2}(t) \tag{A13}$$

A.5. Sine(RF)-modulated pulses

First, we calculate the transmembrane voltage $\Delta\Phi_{\mathrm{msin}}$ induced by a sine-shaped $E(t)$:

$$E(t)=\sin\omega t\cdot u_0(t) \tag{A14a}$$

$$E(s)=\frac{\omega}{s^2+\omega^2} \tag{A14b}$$

$$\frac{\Delta\Phi_{\mathrm{msin}}(s)}{R}=\frac{\omega(a_1+a_2s+a_3s^2)}{(b_1+b_2s+b_3s^2)(s^2+\omega^2)} \tag{A14c}$$

$$
\begin{aligned}
\frac{\Delta\Phi_{\mathrm{msin}}(t)}{R} = {} & \frac{a_1 b_1 + (a_2 b_2 - a_1 b_3 - a_3 b_1)\,\omega^2 + a_3 b_3 \omega^4}{b_1^2 + \left(b_2^2 - 2 b_1 b_3\right)\omega^2 + b_3^2 \omega^4} \cdot \sin \omega t \cdot u_0(t) \\
& + \frac{(a_2 b_1 - a_1 b_2)\,\omega + (a_3 b_2 - a_2 b_3)\,\omega^3}{b_1^2 + \left(b_2^2 - 2 b_1 b_3\right)\omega^2 + b_3^2 \omega^4} \cdot \cos \omega t \cdot u_0(t) \\
& + \left[\frac{\dfrac{a_1 b_2}{2} - \dfrac{a_2 b_1}{2} + \dfrac{a_3 b_1^2 - a_1 b_1 b_3 - \dfrac{a_2 b_1 b_2}{2} + \dfrac{a_1 b_2^2}{2}}{\sqrt{b_2^2 - 4 b_1 b_3}}}{b_1^2 + \left(b_2^2 - 2 b_1 b_3\right)\omega^2 + b_3^2 \omega^4} \right. \\
& \left. + \frac{\dfrac{a_2 b_3}{2} - \dfrac{a_3 b_2}{2} + \dfrac{a_1 b_3^2 - a_3 b_1 b_3 - \dfrac{a_2 b_2 b_3}{2} + \dfrac{a_3 b_2^2}{2}}{\sqrt{b_2^2 - 4 b_1 b_3}}}{b_1^2 + \left(b_2^2 - 2 b_1 b_3\right)\omega^2 + b_3^2 \omega^4}\, \omega^2 \right] \cdot \omega \cdot e^{-\frac{t}{\tau_1}} \cdot u_0(t) \\
& + \left[\frac{\dfrac{a_1 b_2}{2} - \dfrac{a_2 b_1}{2} - \dfrac{a_3 b_1^2 - a_1 b_1 b_3 - \dfrac{a_2 b_1 b_2}{2} + \dfrac{a_1 b_2^2}{2}}{\sqrt{b_2^2 - 4 b_1 b_3}}}{b_1^2 + \left(b_2^2 - 2 b_1 b_3\right)\omega^2 + b_3^2 \omega^4} \right. \\
& \left. + \frac{\dfrac{a_2 b_3}{2} - \dfrac{a_3 b_2}{2} - \dfrac{a_1 b_3^2 - a_3 b_1 b_3 - \dfrac{a_2 b_2 b_3}{2} + \dfrac{a_3 b_2^2}{2}}{\sqrt{b_2^2 - 4 b_1 b_3}}}{b_1^2 + \left(b_2^2 - 2 b_1 b_3\right)\omega^2 + b_3^2 \omega^4}\, \omega^2 \right] \cdot \omega \cdot e^{-\frac{t}{\tau_2}} \cdot u_0(t). \qquad \text{(A14d)}
\end{aligned}
$$

To obtain a response to a sine-modulated step function, we add the step response to the calculated response:

$$\Delta\Phi_{\mathrm{msmp}} = \Delta\Phi_{\mathrm{msin}} + \Delta\Phi_{\mathrm{m1}} \qquad \text{(A15)}$$

where it is presumed that both responses have already been scaled: $\Delta\Phi_{\mathrm{msin}}$ by R and the amplitude of sine-shaped $E(t)$, and $\Delta\Phi_{\mathrm{m1}}$ by R and the amplitude of step-shaped $E(t)$. To get a response to a sine-modulated pulse with duration T_1, we simply have to take the response given by Eq. (A15), and subtract an equivalent response at $t = T_1$:

$$\Delta\Phi_{\mathrm{m}}(t) = \Delta\Phi_{\mathrm{msmp}}(t) \cdot u_0(t) - \Delta\Phi_{\mathrm{msmp}}(t - T_1) \cdot u_{T_1}(t). \qquad \text{(A16)}$$

The response to a train of sine-modulated pulses is then calculated using the principle from Eq. (A8).

A.6. Possible simplifications of the calculated expressions

Using a computer, one can easily evaluate the expressions given in the preceding subsections. Nevertheless, when realistic values of the parameters are considered, these suggest several possibilities for simplifications. Firstly, membrane conductivity is by several orders of magnitude smaller compared to the conductivities of the cytoplasm and the extracellular medium (see Table 1):

$$\lambda_{\mathrm{m}} \ll \lambda_{\mathrm{i}}, \lambda_{\mathrm{o}}. \qquad \text{(A17)}$$

Secondly, membrane thickness is about a thousand-fold smaller than cell radius:

$$d \ll R \tag{A18}$$

One generally justifiable simplification emerges from a thorough analysis of expressions in Eqs. (A6d), (A9d), (A12d) and (A14d). Using realistic values of the parameters (see Table 1), it shows that the amplitude of the exponential term involving τ_2 is always much smaller (at least four orders of magnitude) than the amplitude of the term involving τ_1. Thus, the partial response pertaining to τ_2 can be neglected without serious consequences, giving the system an apparent first-order nature.

Based on Eqs. (A17) and (A18), some terms in the expressions describing a_1, a_2, a_3, b_1, b_2, and b_3, given by Eqs. (9a), (9b), (9c), (9d), (9e) and (9f), appear negligible in comparison to the others. One should, however, be very careful when deciding to eliminate these terms. Since the apparently largest terms often cancel out after a full expansion of the expression, the seemingly negligible terms that include d, or λ_m, sometimes play a major role in determination of the response. An example of an invalid simplification can be illustrated using expression for τ_1, given by Eq. (A6e); if expressions describing b_1, b_2 and b_3 are primarily modified by eliminating the terms involving λ_m, and then inserted into Eq. (A6e), the computation yields $\tau_1 = 0$, which is obviously wrong. If, however, all the terms are retained until the expression is fully expanded, and the approximations are applied to this expression, one obtains a solution which yields a more plausible estimation of τ_1 (due to the size of the expanded expression, we avoid its explicit formulation here). Commonly, an additional postulation is used that both the extracellular medium and the cytoplasm are purely conductive:

$$\varepsilon_i = \varepsilon_o = 0. \tag{A19}$$

As all the terms involving ε_i and ε_o are left out, the size of the expression is vastly reduced. Though in case of a general system, the appropriateness of this procedure may be questioned, when used with the parameter values representative for a cell suspension, the resulting expression

$$\tau_1 = \frac{R\varepsilon_m(\lambda_i + 2\lambda_o)}{R\lambda_m(\lambda_i + 2\lambda_o) + 2d\lambda_i\lambda_o} \tag{A20}$$

can be shown to never deviate more than 2% from the complete expression given by Eq. (A6e).

Expressing ε_m/d as membrane capacitance (c_m) yields the well-known expression for the time constant of the membrane as given by Pauly and Schwan [11]:

$$\tau_1 = \frac{Rc_m}{\dfrac{2\lambda_i\lambda_o}{\lambda_i + 2\lambda_o} + \dfrac{R}{d}\lambda_m}. \tag{A21}$$

References

[1] K.R. Robinson, The responses of cells to electrical fields, J. Cell Biol. 101 (1985) 2023–2027.

[2] P. Marszalek, D.S. Liu, T.Y. Tsong, Schwan equation and transmembrane potential induced by alternating electric field, Biophys. J. 58 (1990) 1053–1058.

[3] T.Y. Tsong, Electroporation of cell membranes, Biophys. J. 60 (1991) 297–306.

[4] W. Krassowska, J.C. Neu, Response of a single cell to an external electric field, Biophys. J. 66 (1994) 1768–1776.

[5] E. Neumann, A.E. Sowers, C.A. Jordan (Eds.), Electroporation and Electrofusion in Cell Biology, Plenum, New York, 1989.

[6] D.C. Chang, B.M. Chassy, J.A. Saunders, A.E. Sowers (Eds.), Guide to Electroporation and Electrofusion, Academic Press, San Diego, 1992.

[7] T.K. Wong, E. Neumann, Electric field mediated gene transfer, Biochem. Biophys. Res. Commun. 107 (2) (1982) 584–587.

[8] M.M.S. Lo, T.Y. Tsong, M.K. Conrad, S.M. Strittmatter, L.D. Hester, S. Snyder, Monoclonal antibody production by receptor-mediated electrically induced cell fusion, Nature 310 (1984) 792–794.

[9] M. Okino, H. Mohri, Effects of a high-voltage electrical impulse and an anticancer drug on in vivo growing tumors, Jpn. J. Cancer Res. 78 (1987) 1319–1321.

[10] T. Kotnik, F. Bobanović, D. Miklavčič, Sensitivity of transmembrane voltage induced by applied electric fields – a theoretical analysis, Bioelectrochem. Bioenerg. 43 (1997) 285–291.

[11] H. Pauly, H.P. Schwan, Über die Impedanz einer Suspension von kugelförmigen Teilchen mit einer Schale, Z. Naturforsch., B: Anorg. Chem., Org. Chem. 14 (1959) 125–131.

[12] D. Šemrov, D. Miklavčič, Calculation of the electrical parameters in electrochemotherapy of solid tumors in mice, Comput. Biol. Med. (in press).

[13] R.M. Fano, L.J. Chu, R.B. Adler, Electromagnetic Fields, Energy, and Forces, Wiley, New York, 1960.

[14] R.V. Churchill, Operational Mathematics, McGraw-Hill, New York, 1972.

[15] M. Hibino, H. Itoh, K. Kinosita Jr., Time courses of electroporation as revealed by submicrosecond imaging of transmembrane potential, Biophys. J. 64 (1993) 1789–1800.

[16] G. Fuhr, F. Geissler, T. Müller, R. Hagedorn, H. Torner, Differences in the rotation spectra of mouse oocytes and zygotes, Biochim. Biophys. Acta 930 (1987) 65–71.

[17] W.M. Arnold, R.K. Schmutzler, A.G. Schmutzler, H. van der Ven, S. Al-Hasani, D. Krebs, U. Zimmermann, Electrorotation of mouse oocytes: single-cell measurements of zona-intact and zona-free cells and of the isolated zona pellucida, Biochim. Biophys. Acta 905 (1987) 454–464.
[18] K. Asami, T. Hanai, N. Koizumi, Dielectric properties of yeast cells, J. Membr. Biol. 28 (1976) 169–180.
[19] C.M. Harris, D.B. Kell, The radio-frequency dielectric properties of yeast cells measured with a rapid, automated, frequency-domain dielectric spectrometer, Bioelectrochem. Bioenerg. 11 (1983) 15–28.
[20] R. Hölzel, I. Lamprecht, Dielectric properties of yeast cells as determined by electrorotation, Biochim. Biophys. Acta 1104 (1992) 195–200.
[21] P.R.C. Gascoyne, R. Pethig, J.P.H. Burt, F.F. Becker, Membrane changes accompanying the induced differentiation of Friend murine erythroleukemia cells studied by dielectrophoresis, Biochim. Biophys. Acta 1146 (1993) 119–126.
[22] X. Hu, W.M. Arnold, U. Zimmermann, Alterations in the electrical properties of T and B lymphocyte membranes induced by mitogenic stimulation: activation monitored by electrorotation of single cells, Biochim. Biophys. Acta 1021 (1990) 191–200.
[23] D. Wicher, J. Gundel, Electrorotation of multi- and oligolamellar liposomes, Bioelectrochem. Bioenerg. 21 (1989) 279–288.
[24] C. Grosse, H.P. Schwan, Cellular membrane potentials induced by alternating fields, Biophys. J. 63 (1992) 1632–1642.
[25] G. Fuhr, R. Glaser, R. Hagedorn, Rotation of dielectrics in a rotating electric high-frequency field, Biophys. J. 49 (1986) 395–402.
[26] K.V.I.S. Kaler, T.B. Jones, Dielectrophoretic spectra of single cells determined by feedback-controlled levitation, Biophys. J. 57 (1990) 173–182.
[27] J. Gimsa, R. Glaser, G. Fuhr, in: W. Schutt, H. Klinkmann, I. Lamprecht, T. Wilson (Eds.), Physical Characterization of Biological Cells, Verlag Gesundheit, Berlin, 1991, pp. 295–323.
[28] B. Alberts, D. Bray, J. Lewis, M. Raff, K. Roberts, J.D. Watson, Molecular Biology of the Cell, Garland Publishing, New York, 1994.
[29] E. Tekle, R.D. Astumian, P.B. Chock, Selective and asymmetric molecular transport across electroporated cell membranes, Proc. Natl. Acad. Sci. U.S.A. 91 (1994) 11512–11516.
[30] S. Kakorin, S.P. Stoylov, E. Neumann, Electro-optics of membrane electroporation in diphenylhexatriene-doped lipid bilayer vesicles, Biophys. Chem. 58 (1996) 109–116.
[31] A.E. Sowers, in: E. Neumann, A.E. Sowers, C.A. Jordan (Eds.), Electroporation and Electrofusion of Cell Membranes, Plenum, New York, 1989, pp. 229–256.
[32] T.C. Tomov, Quantitative dependence of electroporation on the pulse parameters, Bioelectrochem. Bioenerg. 37 (1995) 101–107.
[33] U. Pliquett, E.A. Gift, J.C. Weaver, Determination of the electric field and anomalous heating caused by exponential pulses with aluminum electrodes in electroporation experiments, Bioelectrochem. Bioenerg. 39 (1996) 39–53.
[34] D.C. Chang, Cell poration and cell fusion using an oscillating electric field, Biophys. J. 56 (1989) 641–652.
[35] D.C. Chang, P.Q. Gao, B.L. Maxwell, High efficiency gene transfection by electroporation using a radio-frequency electric field, Biochim. Biophys. Acta 1092 (1991) 153–160.
[36] K.M. Merz Jr., B. Roux, in: K.M. Merz Jr., B. Roux (Eds.), Biological Membranes: A Molecular Perspective from Computation and Experiment, Birkhäuser, Boston, 1996, p. viii.
[37] J.C. Weaver, Y.A. Chizmadzhev, Theory of electroporation: a review, Bioelectrochem. Bioenerg. 41 (1996) 135–160.
[38] H. Fröhlich, Theory of Dielectrics, Clarendon Press, Oxford, 1986.
[39] P.R.C. Gascoyne, F.F. Becker, X.B. Wang, Numerical analysis of the influence of experimental conditions on the accuracy of dielectric parameters derived from electrorotation measurements, Bioelectrochem. Bioenerg. 36 (1995) 115–125.